

Gradient filters based on the fast wavelet transform for quasi-identical noisy images

S.M. Prigarin

Abstract. The paper deals with a family of nonlinear gradient filters that can be applied to one noisy image or several quasi-identical patterns (i.e., several images of the same object with independent noise). Such filters are based on a specific wavelet decomposition and a preliminary statistical analysis of quasi-identical patterns. Results of numerical experiments have shown that the developed gradient filters reduce noise and preserve image boundaries.

Introduction

A multiple image denoising method (MID) was proposed in [1] for the noise reduction in medical x-ray imaging based on two quasi-identical patterns. The main idea underlying the method is to make several x-ray images of the same object and produce a resulting image of a better quality by specialized filtering along with minimizing the total dose of radiation [2]. The MID algorithm is based on the fast wavelet transform described in [3]. The authors of [1] demonstrate the availability of the MID method by several examples and mention a negative effect: random low-contrast blotches can appear in the resulting image.

The main goal of this paper is to improve the original MID algorithm eliminating appearance of blotches. As a result, a family of gradient filters was developed and enhanced modifications of the MID algorithms were proposed.

1. Wavelet transform and MID algorithm

The MID algorithm described in [1, 4] is based on the fast wavelet transform from [3]. This fast wavelet transform is presented below.

Let $I = I_0$ be a grey $N \times N$ -image, $I = [I(n, m)]_{n, m=1, \dots, N}$. The wavelet transform of the image I_0 can be written down in the form

$$W_{j+1}^{(1)} = I_j * (G_j, D), \quad W_{j+1}^{(2)} = I_j * (D, G_j), \quad I_{j+1} = I_j * (H_j, H_j), \quad (1) \\ j = 0, \dots, J - 1.$$

The inverse wavelet transform (the reconstruction algorithm) is the following

$$I_{j-1} = W_j^{(1)} * (K_{j-1}, L_{j-1}) + W_j^{(2)} * (L_{j-1}, K_{j-1}) + I_j * (\tilde{H}_{j-1}, \tilde{H}_{j-1}), \quad (2)$$

$$j = J, \dots, 1.$$

Here $A * (R, C)$ denotes a separable convolution of rows and columns of the image A with 1D filters R and C , respectively. The 1D filters H_0, G_0, K_0, L_0, D are given in Table 1. The discrete filters obtained by setting $2^j - 1$ zeros between each of the coefficients of the filters H_0, G_0, K_0, L_0 are denoted by H_j, G_j, K_j, L_j , respectively. The filter \tilde{H}_j is the filter whose transfer function is a complex conjugate of the transfer function of the filter H_j .

Table 1. Finite impulse response of the filters H_0, G_0, K_0, L_0 , and D

n	H_0	G_0	K_0	L_0	D
-3			0.0078125	0.0078125	
-2			0.0546850	0.0468750	
-1	0.125		0.1718750	0.1171875	
0	0.375	-2	-0.1718750	0.6562500	1
-1	0.375	2	-0.0546850	0.1171875	
-2	0.125		-0.0078125	0.0468750	
-3				0.0078125	

In what follows, the transfer function of a filter will be denoted with asterisk:

$$H^*(\omega) = \sum_n \exp(-i\omega n) H(n).$$

The transfer functions are 2π periodic functions satisfying the following relations:

$$H_0^*(\omega) = e^{i\omega/2} [\cos(\omega/2)]^3, \quad G_0^*(\omega) = 4ie^{i\omega/2} \sin(\omega/2),$$

$$G_0^*(\omega)K_0^*(\omega) + |H_0^*(\omega)|^2 = 1, \quad L_0^*(\omega) = \frac{1 + |H_0^*(\omega)|^2}{2},$$

$$H_j^*(\omega) = H_0^*(2^j\omega), \quad G_j^*(\omega) = G_0^*(2^j\omega),$$

$$K_j^*(\omega) = K_0^*(2^j\omega), \quad L_j^*(\omega) = L_0^*(2^j\omega),$$

$$\tilde{H}_j^*(\omega) = \overline{H_j^*(\omega)}.$$

The filters correspond to a quadratic spline wavelet (with the cubic spline derivative, [3, 5]). Border problems are treated by making a symmetry of an image with respect to each of its borders and periodization. The separable convolutions are performed with allowance for this border procedure. At each scale 2^j , algorithm (1) decomposes I_j into I_{j+1} , $W_{j+1}^{(1)}$, and $W_{j+1}^{(2)}$,

while the inverse wavelet transform (2) reconstructs I_{j-1} from I_j , $W_j^{(1)}$, and $W_j^{(2)}$. The two-dimensional fields $W_j = (W_j^{(1)}, W_j^{(2)})$ will be called *gradient fields* of level j . The complexity of the direct and the inverse transforms is $O(N^2 \log N)$.

Using the previous notation, the MID method from [1] for the noise reduction in medical x-ray images based on two quasi-identical patterns can be described in the following way. Let $I[1] = I_0[1]$ and $I[2] = I_0[2]$ be two noisy realizations of the same image I . Consider wavelet transform (1) for these two images:

$$\begin{aligned} W_{j+1}^{(1)}[k] &= I_j[k] * (G_j, D), & W_{j+1}^{(2)}[k] &= I_j[k] * (D, G_j), \\ I_{j+1}[k] &= I_j[k] * (H_j, H_j), & j &= 0, \dots, J-1, \quad k = 1, 2. \end{aligned}$$

This is the first (decomposition) stage of the MID method: generation of the “smoothed” fields $I_J[1]$, $I_J[2]$ of level J and the gradient fields

$$W_j[1] = (W_j^{(1)}[1], W_j^{(2)}[1]), \quad W_j[2] = (W_j^{(1)}[2], W_j^{(2)}[2]) \quad (3)$$

of levels $j = 1, \dots, J$ for both quasi-identical images.

The second (reconstruction) stage of the MID method can be divided into several steps:

Step 1. Pixel-wise averaging of the two smoothed images of level J ,

$$I(J) = (I_J[1] + I_J[2])/2.$$

Set $j = J$.

Step 2. Computing the new gradient fields $W_j^{(1)}$, $W_j^{(2)}$ by the following assignments:

Step 2a. Averaging of the gradient fields

$$W_j'(n, m) = \frac{W_j[1](n, m) + W_j[2](n, m)}{2}.$$

Here (n, m) denotes a pixel with the indices n , m .

Step 2b. Multiplication of the average gradient field by the weights

$$W_j''(n, m) = W_j'(n, m) * P_j(n, m),$$

where the weights $P_j(n, m)$ are computed for every pixel by the formulas

$$P_j(n, m) = \frac{s}{s_1 s_2},$$

$$s = W_j^{(1)}[1](n, m)W_j^{(1)}[2](n, m) + W_j^{(2)}[1](n, m)W_j^{(2)}[2](n, m),$$

$$s_k^2 = (W_j^{(1)}[k](n, m))^2 + (W_j^{(2)}[k](n, m))^2, \quad k = 1, 2,$$

for $s > 0$, and $P_j(n, m) = 0$, otherwise. Here s is a scalar product of the two-dimensional gradient vectors $W[1](n, m)$ and $W[2](n, m)$ at pixel (n, m) , while s_k are the Euclidean norms for the gradient vectors $W[k](n, m)$:

$$s = \langle W_j[1](n, m), W_j[2](n, m) \rangle, \quad s_k = |W_j[k](n, m)|, \quad k = 1, 2.$$

Step 2c. Renormalization of the gradient field

$$W_j = (W_j^{(1)}, W_j^{(2)}) = CW_j'',$$

$$C = \frac{\|U_j'\|^2}{\langle U_j', U_j'' \rangle}. \quad (4)$$

Here

$$U_j' = W_j'^{(1)} * (K_{j-1}, L_{j-1}) + W_j'^{(2)} * (L_{j-1}, K_{j-1}),$$

$$U_j'' = W_j''^{(1)} * (K_{j-1}, L_{j-1}) + W_j''^{(2)} * (L_{j-1}, K_{j-1}),$$

$$\langle U', U'' \rangle = \sum_{n, m} U'(n, m)U''(n, m), \quad \|U\|^2 = \langle U, U \rangle.$$

Formula (4) is used only for $j > 1$ and $\langle U_j', U_j'' \rangle$ larger than 0, otherwise $C = 1$.

Step 3.

$$I_{j-1} = W_j^{(1)} * (K_{j-1}, L_{j-1}) + W_j^{(2)} * (L_{j-1}, K_{j-1}) + I_j * (\tilde{H}_{j-1}, \tilde{H}_{j-1}).$$

Step 4. Cycling: $j = j - 1$, and if $j > 1$, then go to Step 2.

The reconstruction stage of the MID method generates the sequence

$$I_J, W_J, I_{J-1}, W_{J-1}, \dots, I_1, W_1, I_0$$

from the “smoothed” fields $I_J[1], I_J[2]$ and the gradient fields $W_j[1], W_j[2]$, $j = 1, \dots, J$. The image I_0 is the final reconstruction of the image I .

Remark. Renormalization of Step 2c was proposed by one of the authors of paper [1]. But the analysis of filtering results showed that with this step instead of denoising, the noise intensity can be even increased in spite of illusion of a better contrast. Particularly, for the first test described below in Section 3, the empirical variance after the MID filtering with Step 2c is approximately twice as larger as that of the noisy input images. That is the reason why in further considerations Step 2c will be eliminated. Formally it will be assumed that $C = 1$ for Step 2c of the MID algorithm (all the results presented in Section 3 were obtained under this assumption).

2. Gradient filters and modifications of the MID

Image filters with the same general scheme as for the MID algorithm but with a nonlinear filter NLF

$$W_j = NLF(W_j[1], W_j[2]) \quad (5)$$

instead of Step 2 will be called *gradient filters* because the basis of such a filter is a nonlinear transformation (5) of gradient fields (3).

Several gradient filters were considered as a modification of the MID method to eliminate the blotch effect and to improve reduction of noise. One of them (it will be denoted as MID2) is presented below.

Step 2 of MID2 modification. Step 2a is the same as for MID:

$$W'_j(n, m) = \frac{W_j[1](n, m) + W_j[2](n, m)}{2}.$$

Step 2b. The notation $W^{/s,t/}$ will be used for $/s, t/$ -shift of the gradient field W :

$$W^{/s,t/}(n, m) = W(n + s, m + t).$$

For all eight shifts $/s, t/$ from the set

$$\{/0, 1/, /0, -1/, /1, 0/, /-1, 0/, /1, 1/, /-1, 1/, /1, -1/, /-1, -1/\}$$

the following weights are pixel-wise computed by the formula

$$P_j^{/s,t/}(n, m) = \frac{\langle W_j(n, m), W_j^{/s,t/}(n, m) \rangle}{|W_j(n, m)| |W_j^{/s,t/}(n, m)|}$$

if $\langle W_j(n, m), W_j^{/s,t/}(n, m) \rangle > 0$, and $P_j^{/s,t/}(n, m) = 0$, otherwise. The result of this step of the algorithm is a smoothed gradient field

$$W_j''(n, m) = W_j'(n, m) \frac{1}{8} \sum_{/s,t/} P_j^{/s,t/}(n, m),$$

where summation is performed over eight shifts $/s, t/$.

Step 2c. Renormalization of the gradient field $W_j = CW_j''$, where

$$C = \frac{\max_{n,m} |W_j'(n, m)|}{\max_{n,m} |W_j''(n, m)|},$$

for $j > 1$ and $\max_{n,m} |W_j''(n, m)| > 0$, otherwise $C = 1$.

The idea underlying the next modification **MID3** of the gradient filter is to estimate the noise intensity from a difference between two quasi-identical realizations.

Step 2 for MID3 contains the same Steps 2a, 2b, 2c as for MID2 and an additional Step 2b* between Steps 2b and 2c.

Step 2b* for **MID3**. First, the empirical variances

$$v^{(1)} = \frac{1}{N^2} \sum_{n,m} \left(W_j^{(1)}[1](n, m) - W_j^{(1)}[2](n, m) \right)^2 \approx \mathbf{V}(W_j^{(1)}[1] - W_j^{(1)}[2]),$$

$$v^{(2)} = \frac{1}{N^2} \sum_{n,m} \left(W_j^{(2)}[1](n, m) - W_j^{(2)}[2](n, m) \right)^2 \approx \mathbf{V}(W_j^{(2)}[1] - W_j^{(2)}[2])$$

should be computed. Here it is important that the two images are quasi-identical, because in this case the differences $W_j^{(1)}[1] - W_j^{(1)}[2]$ and $W_j^{(2)}[1] - W_j^{(2)}[2]$ are homogeneous random fields with zero mean (under assumption that the noise is statistically homogeneous with the same properties for both images). Then we set

$$W_j''^{(1)}(n, m) = 0 \quad \text{if } |W_j'(n, m)| < \sqrt{C_0 v^{(1)}},$$

and

$$W_j''^{(2)}(n, m) = 0 \quad \text{if } |W_j'(n, m)| < \sqrt{C_0 v^{(2)}}.$$

In other words, we set gradient values to zero if the values are in agreement with noise intensity. A disadvantage of this additional Step 2b* is that a constant C_0 must be defined. But most probably, the value of this constant is more or less universal and can be fixed in an appropriate way for most of medical images.

Remarks. 1. Gradient filters can be combined with additional filtering. The tests have shown that the median filtering can be effective, for instance, after applying the MID3 method (see Figure 7 in the next section). The following regularization of gradient fields seems to be reasonable at every level j . One pixel will be called 'co-directed' with another one if the angle between gradients for these pixels is less than 90 degrees. For every pixel we count its number of co-directed pixels among the nearest eight neighbors. If the number of co-directed neighbors does not exceed a parameter K (typical values are $K = 0, 1, 2$), then for that pixel we take a new value of the gradient, computed as an average of gradients for non co-directed neighboring pixels.

2. Obviously, algorithms MID2 and MID3 can be applied to several quasi-identical patterns as well as to a unique image. A specific feature of these modifications in comparison with the original MID method is a nonlinear smoothing of gradient fields over the nearest 8-pixel neighborhood.

3. Test results and conclusion

In the first test the images $I[1]$, $I[2]$ are independent (250×250) -realizations of the Gaussian white noise with zero mean and unit variance. The empirical mean values and variances for the origin images and after filtering are presented in Table 2.

Table 2. Results for testing of two white noise images

Image	Empirical mean	Empirical variance	Square root of empirical variance
$I[1]$	0.00050	1.0042	1.002
$I[2]$	0.00050	1.0071	1.0035
MID	0.00046	0.2320	0.482
MID2	0.00056	0.0773	0.278
MID3, $C_0 = 0.5$	0.00056	0.0359	0.189

For the second test, a true image was an image of size 200×200 pixels with constant values along one axis and with the profile shown in Figure 1 along another axis. Two quasi-identical patterns were simulated by adding two independent realizations of the Gaussian white noise with zero mean and unit variance (Figures 2, 3). Results for the corresponding profiles and different filters are presented in Figures 4–7.

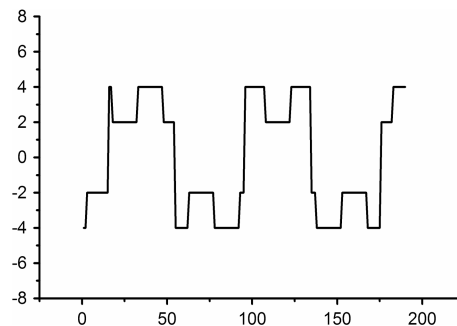


Figure 1. Profile of a true image

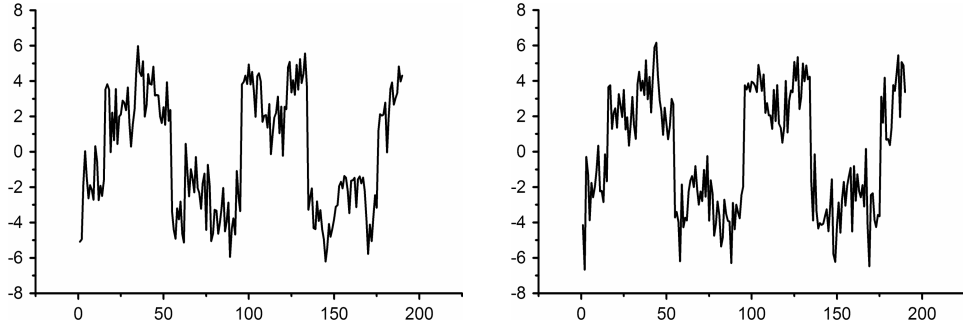


Figure 2. Two profiles of the first quasi-identical pattern $I[1]$

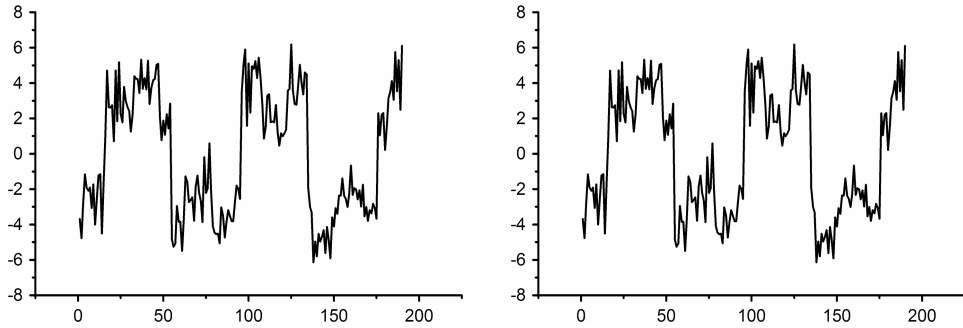


Figure 3. Two profiles of the second quasi-identical pattern $I[2]$

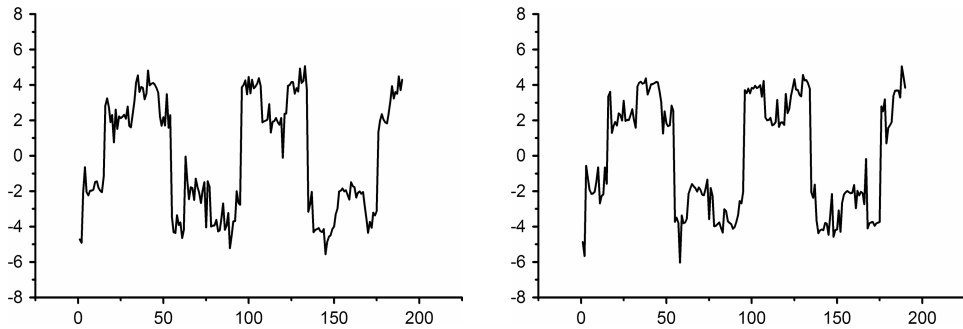


Figure 4. The two profiles after the MID filtering

Several other tests were performed with filtering quasi-identical patterns including medical x-ray images. The following conclusion can be formulated according to the tests results: (1) gradient filters based on the fast wavelet transform give a challenging tool for the boundary preserving smoothing, (2) modifications MID2 and MID3 essentially improve the original MID algorithm enabling diminishing the noise intensity and eliminate the blotch effect.

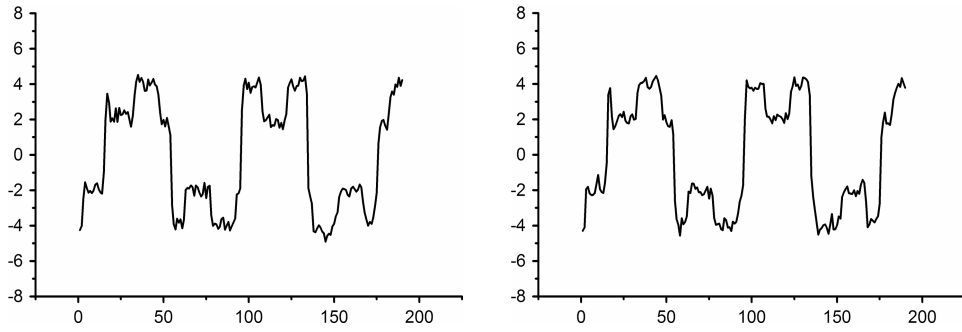


Figure 5. The two profiles after the MID2 filtering

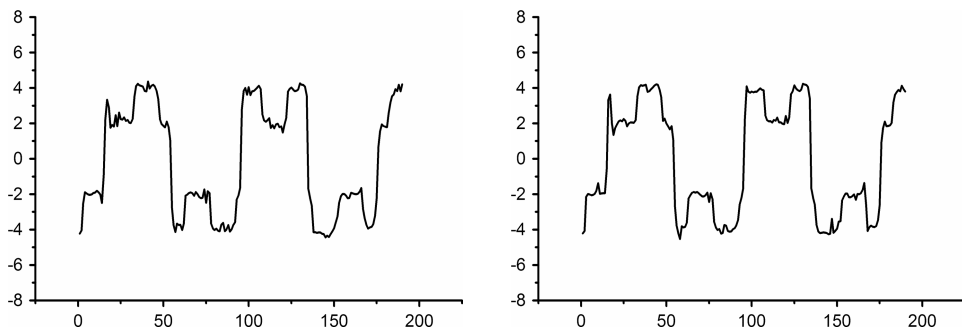


Figure 6. The two profiles after the MID3 filtering, $C_0 = 0.5$

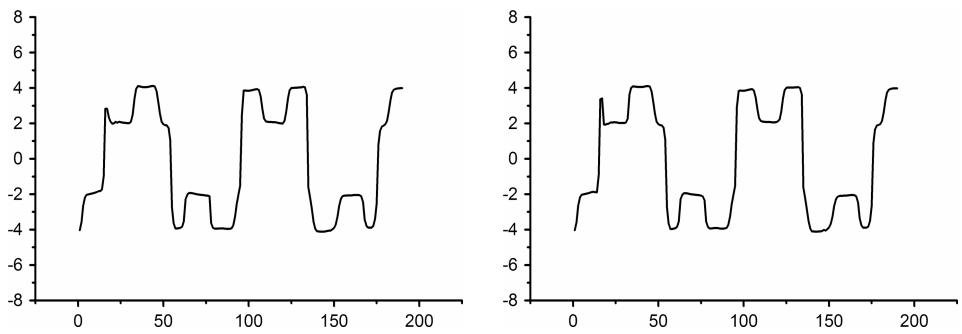


Figure 7. The two profiles after MID3 filtering, $C_0 = 2$, and subsequent 5-point cross median filtering

Acknowledgements. The author would like to thank Dr. Oleg V. Tischenko and Dr. Christoph Höschen for the cooperation and fruitful discussions.

References

- [1] Tischenko O., Hoeschen Ch., Buhr E. Reduction of anatomical noise in medical x-ray images // Radiation Protection Dosimetry. — 2005. — Vol. 114. — P. 69–74.
- [2] Hoeschen C., Tischenko O., Dance D.R., Hunt R.A., Maidment A.D.A., Bakic P.R. Evaluation of a novel method of noise reduction using computersimulated mammograms // Radiat. Prot. Dosim. — 2005. — Vol. 114. — P. 81–84.
- [3] Mallat S., Zhong S. Characterization of signals from multiscale edges // IEEE Transactions on Pattern Analysis and Machine Intelligence. — 1992. — Vol. 14, No. 7. — P. 710–732.
- [4] Tischenko O., Hoeschen Ch., Buhr E. An artifact-free structure-saving noise reduction using the correlation between two images for threshold determination in the wavelet domain // Proc. SPIE. — 2005. — Vol. 5747. — P. 1066–1075.
- [5] Mallat S. A Wavelet Tour of Signal Processing. — Academic Press, 1999.